P2.14 IMPACT OF THE NORTHWEST MEXICAN MONSOON ON PRECIPITATION IN THE CENTRAL UNITED STATES: A MOISTURE AND PV TRANSPORT PERSPECTIVE

Stephen M. Saleeby*
Colorado State University, Ft. Collins, Colorado

William R. Cotton
Colorado State University, Ft. Collins, Colorado

1. INTRODUCTION

Moisture surges from the Gulf of California (GoC) are well known as the northernmost extension of the Mexican monsoon (Douglas et al. 1993, Stensrud et al. 1995). They vary from year to year in duration, intensity, and in the extent of their northward push (Brenner 1974). As surges make their northward progression up the GoC they are known to influence the surface by reducing the temperature and by increasing the mixing ratio, sea level pressure, and southerly winds (Hales 1972, Brenner 1974, Douglas 1993a). Following monsoon onset the low-level reversal in the winds from northwesterly to southerly plays a key role in the transport of low-level moisture northward along the GoC and into the United States (U.S.) (Sadler et al. 1991, Badan-Dagon et al. 1991). Only recently, with better observations and modeling studies, has the prominence of a low-level jet within the GoC been recognized as a primary mechanism for transporting low-level moisture into Arizona (AZ) and New Mexico (NM) (Douglas 1995, Stensrud 1995, 1997). Low-level moisture surges occur periodically throughout the monsoon season and are typically followed by an increase in the amount of rainfall over northwest Mexico and the southwest U.S. Northern Mexico and Arizona often acquire over 60% (Douglas et al. 1993), and 40% (Jurwitz 1953, Bryson and Hare 1974), respectively, of their yearly rainfall from surge events during June-September. The development of surges and their strength is closely tied to the interaction of mid-latitude troughs and tropical easterly waves (Stensrud 1997). It is suggested that the development of the strongest surges occurs if a mid-latitude trough passes the western U.S. a few days prior to the passage of an easterly wave. On the contrary, the simultaneous interaction of these two systems suppresses surge advancement into the southwest U.S. (Stensrud 1997).

With such a large range of variability between surges and the potential for dramatic increases in localized rainfall, understanding the causes and variations in these surges are of great importance for regional forecasts. The RAMS@CSU mesoscale model has been used in this current study to simulate the 1988, 1993, and 1997 monsoon seasons. The primary purpose of this investigation is to gain a better understanding of the linkages between the monsoon and precipitation that occurs on the downstream subsiding branch of the circulation in the central U.S. For the purpose of this paper the focus is on the monsoon onset surge event for the 1993 monsoon season. The 1993 monsoon season began with its first surge event into Arizona on August 3. This onset date was chosen as the onset of the monsoon into the U.S. and is marked as the first significant push of high mixing ratio air across the US/Mexico border into the U.S. southwest. This moisture surge event is examined from a potential vorticity (PV) perspective similar to the PV analysis of the development of tropical moisture plumes described by Mecikalski and Tripoli (1998). Investigation into this surge event, from Aug 3 – Aug 10, reveals moisture and precipitation regimes that are dependent upon the large-scale monsoonal flow. We will attempt to delineate two particular precipitation scenarios that become apparent during the lifecycle of individual monsoon surges.

Corresponding author address: Stephen M. Saleeby, Atmospheric Sci Dept., Colorado State Univ, Fort Collins, CO 80523; e-mail: smsaleeb@atmos.colostate.edu

2. MODEL DESCRIPTION

The seasonal monsoon simulations were completed with use of the non-hydrostatic version of the RAMS@CSU model with sigma-z terrain following coordinates (Version 4.3). The model is arranged with a three-grid configuration whose outermost grid (115 x 90 x 36) has a resolution of 120km and covers much of the northwest hemisphere with the center over the southwest US. There are also two nested grids with 40km spacing; one covers Mexico and the western two-thirds of the U.S. (104 x 110 x 36 grid points) and the other covers the east Pacific ITCZ (188 x 59 x 36). The outermost grid is allowed to consume such a large region so as to include the impact of the large-scale circulations that drive the monsoon. The U.S./Mexico grid is the focus region for the monsoonal flow from Mexico that subsequently influences the Great Plains (GP) region of the US. The ITCZ grid is included to better resolve the circulations from the warm tropical Pacific and the influence on monsoon surge events. The model extends vertically into the stratosphere with a vertically stretched grid whose maximum spacing is 1000m at the highest levels; this allows for the presence of more model levels in the boundary layer. The RAMS model is run with single moment liquid and ice phase bulk microphysics (Walko et al. 1995), two-stream Harrington radiation, Kuo convective parameterization, Smagorinski horizontal diffusion, vertically parameterized Mellor-Yamada diffusion, and Klemp-Wilhelmson lateral boundary conditions.

Model initial conditions are assimilated with NCEP reanalysis data, surface observations, rawinsonde data, weekly averaged SSTs, FAO variable soil type, OGE vegetation data, and heterogeneous soil moisture. The soil moisture is estimated using the Antecedent Precipitation Index (API) method, which considers the previous 90 days of daily precipitation. This method was

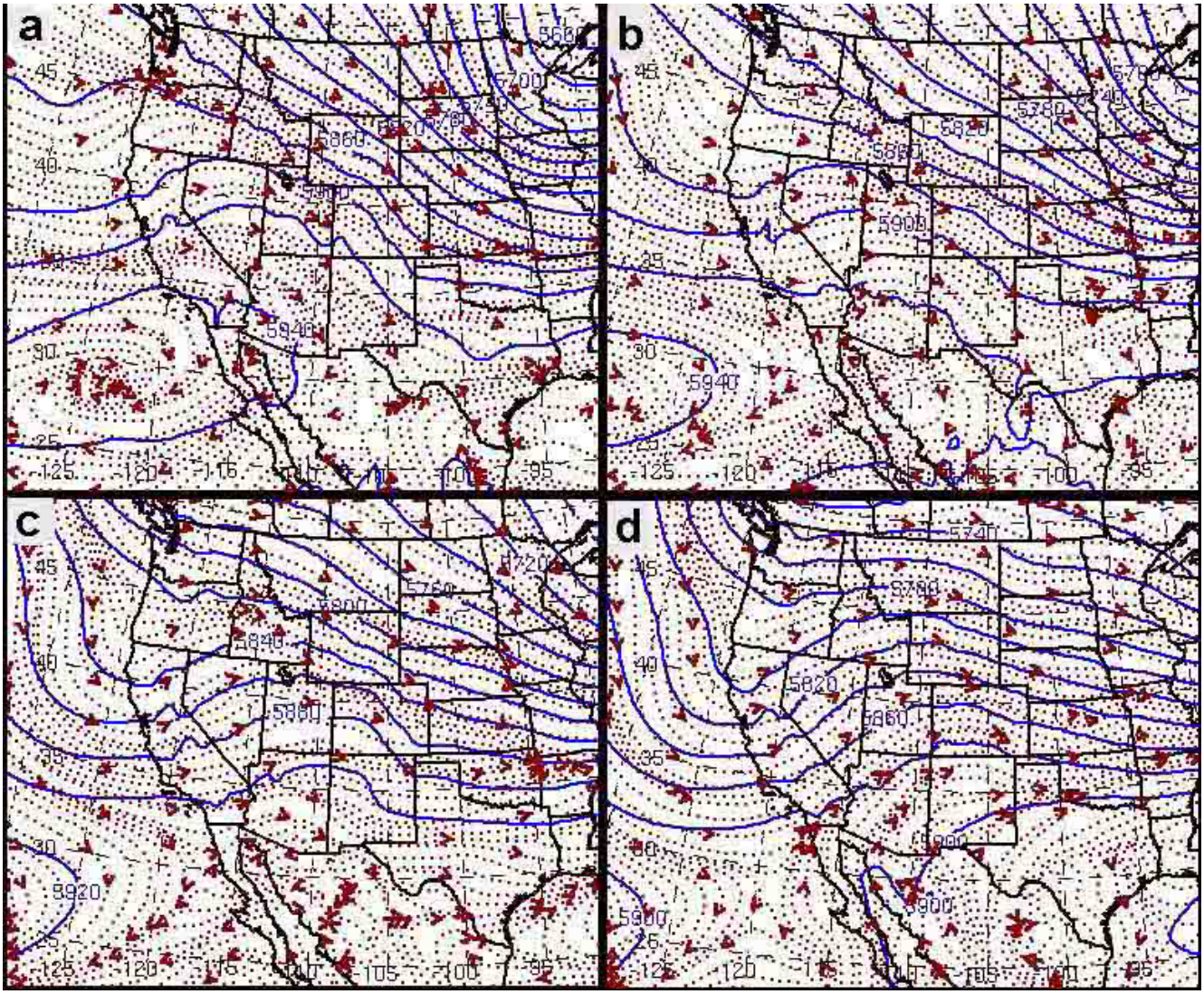

Fig 1. 500mb geopotential height (solid contours, meters) and 500mb streamlines (dotted with arrows) for the following times: a) 6 Aug 0000 UTC, b) 6 Aug 1200 UTC, c) 7 Aug 0000 UTC, and d) 7 Aug1200 UTC.

chosen over other soil moisture products because of the ability to estimate soil moisture over Mexico from a high-density network of daily precipitation gauge data (data provided by Dr. Art Douglas, Creighton University). Many other soil moisture products do not provide data back to 1988 and do not cover areas other than the continental U.S.

Model control simulations were run for the 1988 US drought year (onset June 24), the 1993 US flood year (onset Aug 3), and the 1997 strong El Nino year (onset July 21). The onset dates were determined subjectively and they reflect the first day of the first seasonal monsoon surge that pushes high moisture air across the Mexico/US border into Arizona (AZ) and west New Mexico (NM). The control runs for 1993 and 1997 covered the period from July 1 to August 31 and the 1988 season was run from June 1 to August 15. These chosen periods cover the time from nearly 3 weeks before onset through a number of monsoon surge events in the given season. This was done in order to be able to compare the difference in the flow regimes and the downstream influence before and after the onset of the monsoon, as well as examining individual surge events for patterns that induce the greatest influence on the central U.S. in terms of precipitation.

3. PV APPROACH TO THE MONSOON

The first surge event of 1993 lasted from approximately Aug 3-10. Within this overall surge period there are also daily fluctuations in the strength and northern extent of the surge; this, in turn, influences the daily patterns and intensity of precipitation. In this single surge discussion we will present RAMS model linkages between the shift in the monsoon high and the Pacific trough and the increase in local and downstream anomalies in the moisture, wind, and potential vorticity (PV) fields. Variations of these anomalies are associated with variations in the initiation and maintenance of precipitation systems over the U.S. In establishing such linkages, we attempt to adapt the work of Mecikalski and Tripoli (1997), in which they attribute the formation of tropical plumes to the interaction

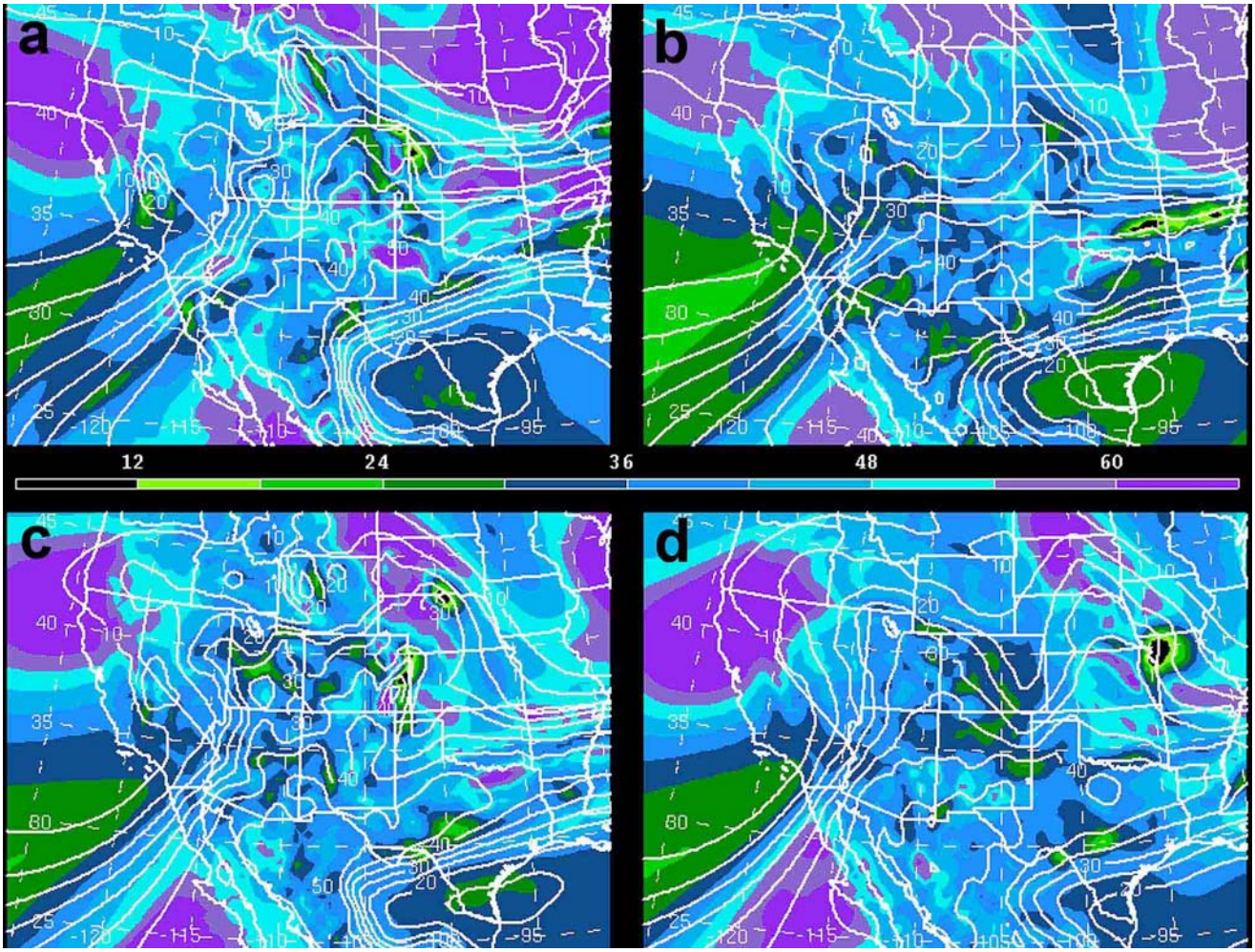

Fig 2. Potential vorticity in the 500mb to 300mb layer (shaded, x 10^8) and 500mb mixing ratio (contoured, g/kg) for the following times: a) 6 Aug 0000 UTC, b) 6 Aug 1200 UTC, c) 7 Aug 0000 UTC, and d) 7 Aug1200 UTC.

of tropical convection zones with a strong sub-tropical trough and a large-scale anti-cyclone over the east Pacific. These flow interactions advect low-valued PV air from near the ITCZ toward the high-valued PV air associated with a deepening trough; this creates a strong PV gradient and a resulting localized jet streak embedded with the large scale flow. They found that the advancing and strengthening trough caused both the formation and demise of the moisture plume.

We will apply an adaptation of this conceptual model to the monsoon cycle to better understand the relationships between the Pacific trough, monsoon anti-cyclone, monsoon moisture, sub-tropical PV anomalies, and precipitation over the GP. Discussion of a sub-cycle of the first monsoon surge event will highlight two classifications of precipitation systems generated during a monsoon burst phase under different flow regimes attributed to strengthening or weakening of the surge. Though only one surge event is discussed in detail, this initial surge is quite representative of other monsoon bursts.

a. Pattern I (6 Aug - 7 Aug)

1. Large-scale features

During the early part of this sub-surge event (Aug 6 00Z), the Pacific trough, shown in the 500mb height and streamline field (Fig 1a), is centered just offshore of the northwest coast. The trough is rather weak and is positioned to the rear of a strong upper-level low that had recently passed through the central U.S. into the Great Lakes region. This strong low-pressure region weakened the influence of the monsoon ridge in the U.S. and forced the anti-cyclone into southern Texas. A sub-tropical high that was originally positioned well west of Baja has shifted eastward with the passage of the low and is aiding in the production of mid-level northwesterly flow across the desert southwest. A region of high-valued PV air in the 500-300mb layer, associated with the trough, is just off the northern California coast, and another region of high-valued PV air is located off of southern Baja and the GoC (Fig 2a). From Aug 6 1200 UTC until Aug 7 1200 UTC the Pacific trough begins to deepen, but remains positioned along the Pacific coast while exhibiting a slight positive tilt (Fig 1b-d).

The monsoon ridge and anti-cyclone begin to show signs of organization as the Pacific trough strengthens and the upper level low pushes east of the Great Lakes. The anti-cyclone is still not very distinct by

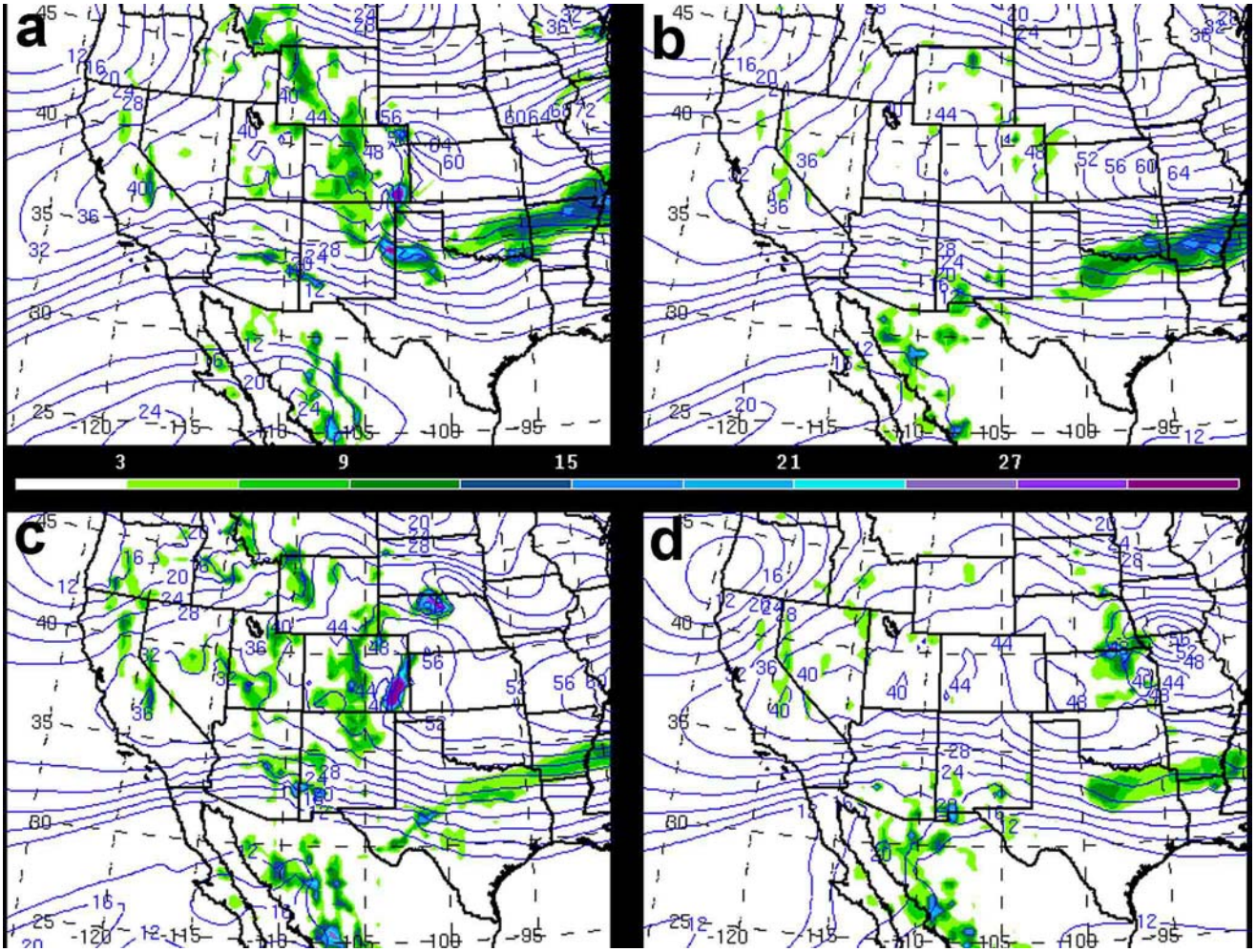

Fig 3. 300mb isotachs (contours, knts) and 500mb vertical velocity (shaded, cm/s) for the following times: a) 6 Aug 0000 UTC, b) 6 Aug 1200 UTC, c) 7 Aug 0000 UTC, and d) 7 Aug1200 UTC.

Aug 7 1200 UTC, but there is a broad scale clockwise circulation along the central Rio Grande. The flow into southern Arizona also becomes more southwesterly as time progresses through 07/1200 UTC. The initial large-scale features in the PV field also persist and maintain their relative magnitudes through 07/1200 UTC, though it is noteworthy that the low-valued PV feature along the southern CA coast is most prominent when the Pacific trough is weakest (Fig 2b-d).

During this two day period the high-valued PV region to the west of Baja shifts slowly northward along the coast so that it is positioned toward the north-central part of Baja by the end of this time period. This shift greatly increases the PV gradient along the northernmost region of Baja between the northern low-valued PV region and the Baja high-valued PV anomaly. This strong gradient region corresponds to an increase in the flow off of the Pacific and the southwesterly shift in the winds.

2. Small-scale Features

While this large-scale pattern is in place, the western mountain states of the U.S. are marked with a more sporadic pattern in the PV field and seemingly unorganized variations in the fields for each time shown in figure 2. Embedded within this less uniform PV field is the daily development of low-valued PV anomalies and mesoscale moisture perturbations associated with deep-convective heating along the front range of the Colorado Rocky Mountains around 0000 UTC on Aug 6 and 7. During their lifecycles the noticeably low-valued anomalies are bounded to the north by regions of high-valued PV air, thereby, creating rather strong mesoscale PV gradients. Such a combination of mid to upper level mesoscale PV features have the ability to produce localized jet streaks embedded within the larger scale jet stream flow, as seen on a larger scale by Mecikalski and Tripoli (1997). The 300mb isotach and 500mb vertical velocity fields (Fig 3) display the formation of jet streaks associated with these PV anomalies. The position of the maxima in vertical velocity in the vicinity of the right, entrance region of the jet streaks suggests that they have developed the secondary circulation and the cross-stream ageostrophic flow that is needed to maintain a balanced and sustained jet streak.

Co-located with these features is the pattern in the surface precipitation rate (Fig 4). At 0000 UTC on both Aug 6 and 7, precipitation persists along the moisture gradient that extends from central AZ through central CO. The combination of strong vertical velocity,

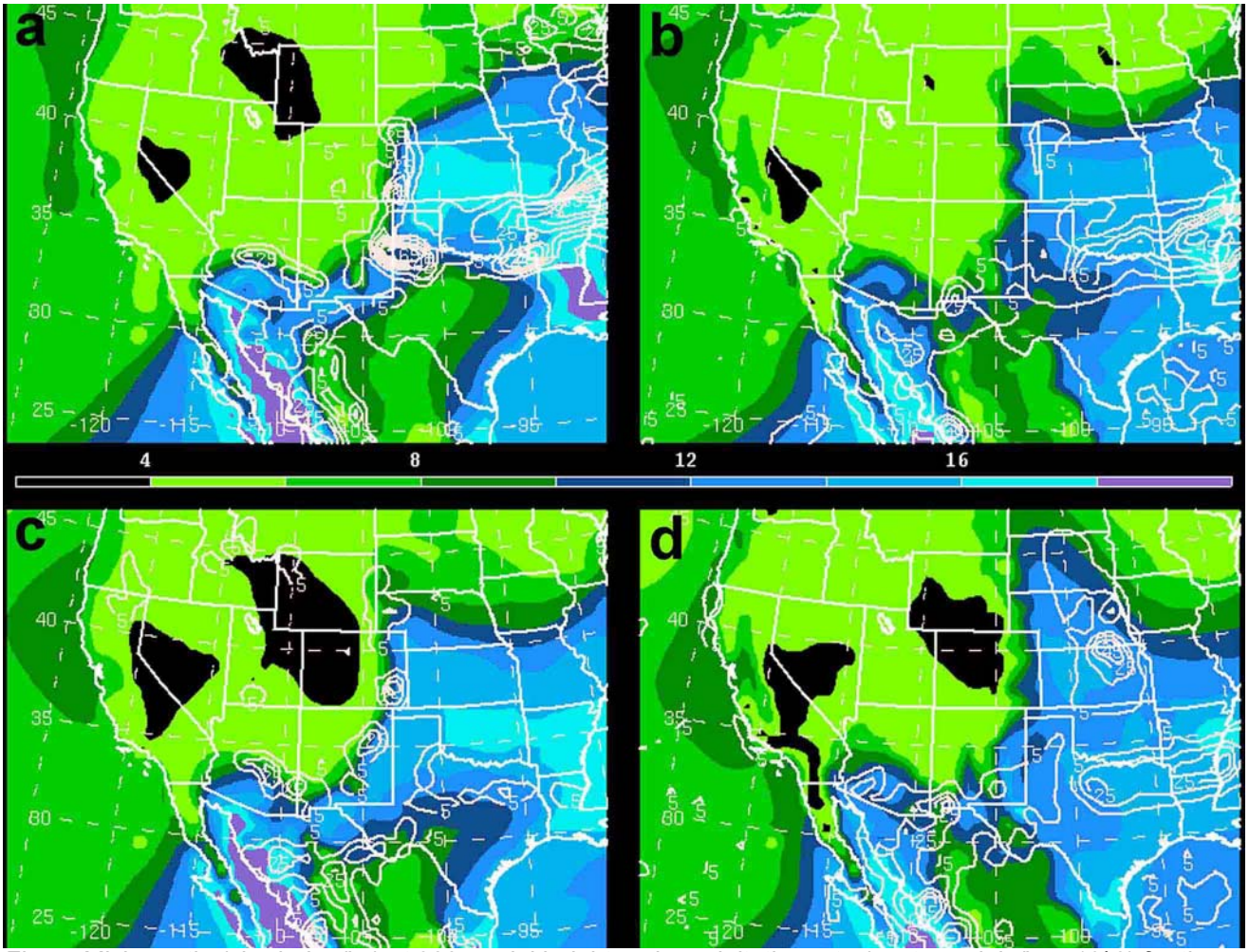

Fig 4. Mixing ratio (shaded, g/kg) at 233 model height and precipitation rate (contoured, in/hr x 10^2) for the following times: a) 6 Aug 0000 UTC, b) 6 Aug 1200 UTC, c) 7 Aug 0000 UTC, and d) 7 Aug1200 UTC.

likely induced by westerly flow over the CO mountains, provides the necessary lift for initiation of convection. As is typical along the front range of the Rockies in CO during the summer months, systems form over the mountains where the vertical velocity is strong and the mid-level source of moisture is in place from the monsoonal flow. These mesoscale systems strengthen once they reach the CO plains and the enhanced low-level moisture (see Fig 4).

The development of the self-contained mesoscale jet circulations from the original PV anomalies aids in lengthening the lifetime of these precipitation systems, though some may be maintained better and longer than others. The original system that developed in northeast CO at 06/0000 UTC is no longer a distinct, separate feature 6-12 hours later. At 06/0600 UTC (not shown) the jet streak is indistinguishable from the strong jet core downstream. The system advects to the southeast by strong upper-level northwesterlies, and it becomes a part of the larger east-west oriented system positioned from central Oklahoma into Arkansas at 06/1200 UTC.

By 07/0000 UTC two significant low-valued PV anomalies develop; one is located in central Nebraska along the South Dakota border and the other is along the eastern plains of CO. Both are co-located with local maxima in the upper-level flow, strong vertical velocity, and localized regions of convection and precipitation. By 07/1200 UTC the two mesoscale systems merge into one distinct system near the Kansas-Missouri border. There is a well-defined region of low-valued PV air, a well-formed jet streak to its northeast with strong vertical motion along the right-entrance region, and a region of heavy precipitation near the southwest gradient region of the PV anomaly. The greatest contributor to this feature is the original low-valued PV in central Nebraska. The PV low in eastern CO weakens by 07/0600 UTC but eventually merges to form the southern end of the low-valued PV anomaly in Missouri at 07/1200 UTC. The merger of these two mesoscale systems is guided by the region of weak confluence in northwest Missouri as seen by the convergence of the 300mb streamlines from Nebraska with the those from southern Kansas. The low-valued PV perturbation in CO first advects toward OK at 07/0000 UTC, but then turns east-northeast by 07/0600 UTC (not shown), at which time it begins to merge with the distinct low-valued PV anomaly to the north.

The final destination of these mesoscale precipitation systems is controlled in part by the location of the monsoon high, the strength of the upper level flow

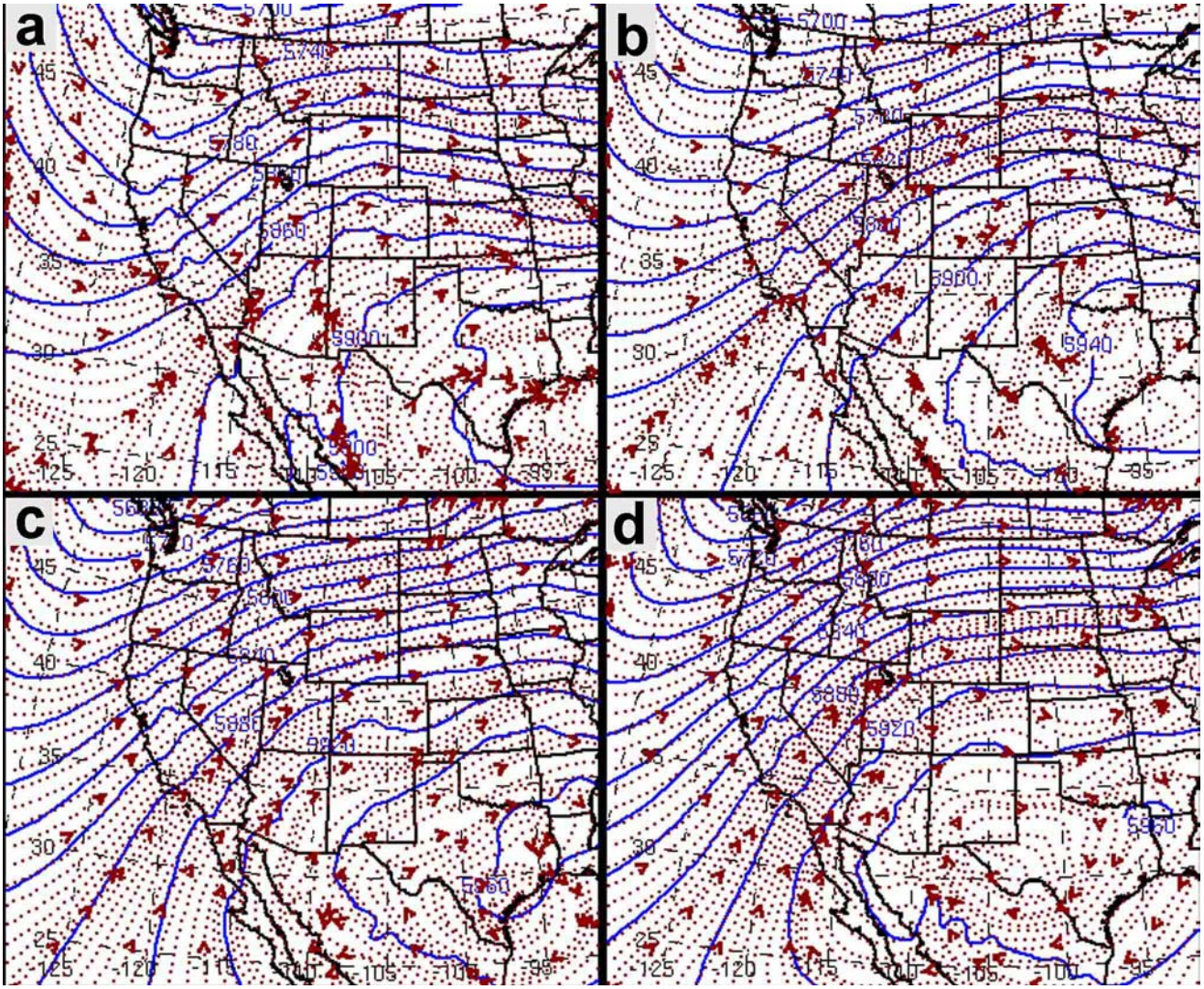

Fig 5. 500mb geopotential height (solid contours, meters) and 500mb streamlines (dotted with arrows) for the following times: a) 8 Aug 0000 UTC, b) 8 Aug 1200 UTC, c) 9 Aug 0000 UTC, and d) 9 Aug1200 UTC.

from the northwest along the backside of the high, and the passage of strong mid-latitude troughs along the northern tier of the US. The system that originates at 06/0000 UTC in CO is quickly influenced by the strong mid-latitude upper-level flow and forced southward into Arkansas by northwesterly flow behind the monsoon high. In contrast, the one that forms from the merger of the PV anomalies in CO and central Nebraska at 07/0000 UTC forms when the upper level flow in the central U.S. is weaker. This system propagates only as far south as Missouri by 07/1200 UTC.

b. Pattern II (8 Aug - 9 Aug)

1. Large-scale features

The large-scale upper-level flow and PV pattern begins to change around 08/0000 UTC. The Pacific trough begins to strengthen and move westward offshore from 08/0000 UTC through 09/1200 UTC (Fig 5). During this time it acquires a positive tilt, extends itself at least as far south as southern Baja, and creates a stronger and more uniform southwesterly flow field along the entire extent of the Pacific coast. The monsoon anti-cyclone also propagates westward back into the domain in the figures and establishes itself into west Texas by 09/1200 UTC. The Pacific coast PV field also undergoes a change as the trough deepens and retreats offshore. The large high-valued PV anomaly that has been in place along the northern California coast since at least 06/0000 UTC loses intensity, elongates into more of a filament, and begins advecting into the northwest US by 08/1200 UTC (Fig 6). The high-valued PV anomaly that slowly made its way northward along the Baja coast also weakens by 08/1200 UTC and advects into the US. The broad region of lower PV air that was sandwiched between these two coastal features also advects into the western US by the increasing Pacific flow. By 09/0000 UTC the PV field along the Pacific coast is marked by a weaker north-south gradient, and the field over the western US is much more uniform than the previous two days. During this transition there is also a shift in the PV pattern over the central U.S. and an apparent change in the source of precipitation for the GP and mid-west. These large-scale changes also contain mesoscale

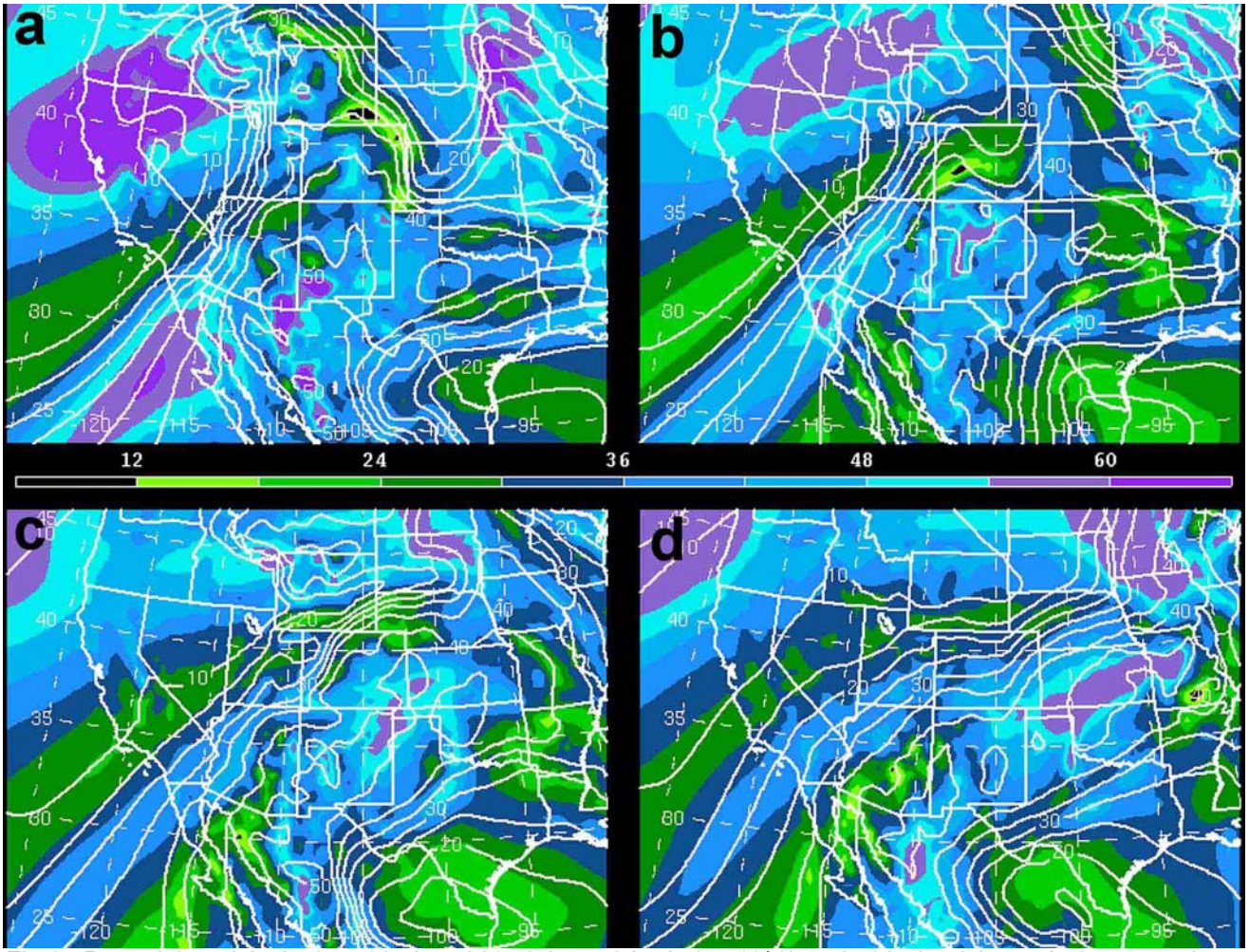

Fig 6. Potential vorticity in the 500mb to 300mb layer (shaded, x 10^8) and 500mb mixing ratio (contoured, g/kg) for the following times: a) 8 Aug 0000 UTC, b) 8 Aug 1200 UTC, c) 9 Aug 0000 UTC, and d) 9 Aug1200 UTC.

features that are on a bit larger spatial scale than the low-valued PV anomalies seen before the transition.

2. Small-scale features

The PV anomaly forming in CO at 08/0000 UTC does not distinctly appear 6-12 hours later, and the tight PV gradients associated with the mesoscale anomalies is not as apparent as in the previous times. During the previous two days, there were small-scale, high-valued PV features over parts of the SMO, but there was little to indicate any organization or coherent propagation of these features. During the weakening of the high-valued PV feature near Baja, though, the SMO high-valued PV anomaly forms and acts as a coherent system that strengthens and advects into the US from 08/0000 to 09/1200 UTC. It propagates and grows in size and strength as it travels from the SMO, through NM and the Texas panhandle, and into Kansas and Missouri by 09/1200 UTC.

The vertical velocity field also reveals significant differences with the change in flow regimes (Fig 7). The strong upward motion that previously appeared downwind of Colorado in conjunction with the PV anomalies and induced jet streaks is diminished without the presence of these features. On the contrary, the average vertical velocity over the SMO appears to have increased slightly. In both cases, the regions of broad scale vertical motion are mostly aligned with the gradient region on the south side of the upper-level jet. With the change from upper-level nearly-zonal flow to anti-cyclonic flow over the central US, the vertical motion field has changed to more closely match the perimeter of the monsoon anti-cyclone. The high-valued PV system that exits the SMO follows a path around the periphery of the monsoon high and is evident in the maximum in the vertical velocity over Missouri at 09/1200 UTC.

The low-level mixing ratio and precipitation rate fields also exhibit noticeable changes. The mixing ratio has its greatest northernmost surge following the deepening and westward movement of the trough and anti-cyclone. Larger values of mixing ratio at the low and mid levels also coincide with the plume that exits the SMO and travels across the lower plains. The low and mid-level moisture in CO pushes eastward so that the mountains are left without the moisture source that was present during the development phase of the convective systems on Aug 6-7. The precipitation field reflects these changes such that the rainfall is diminished in CO and

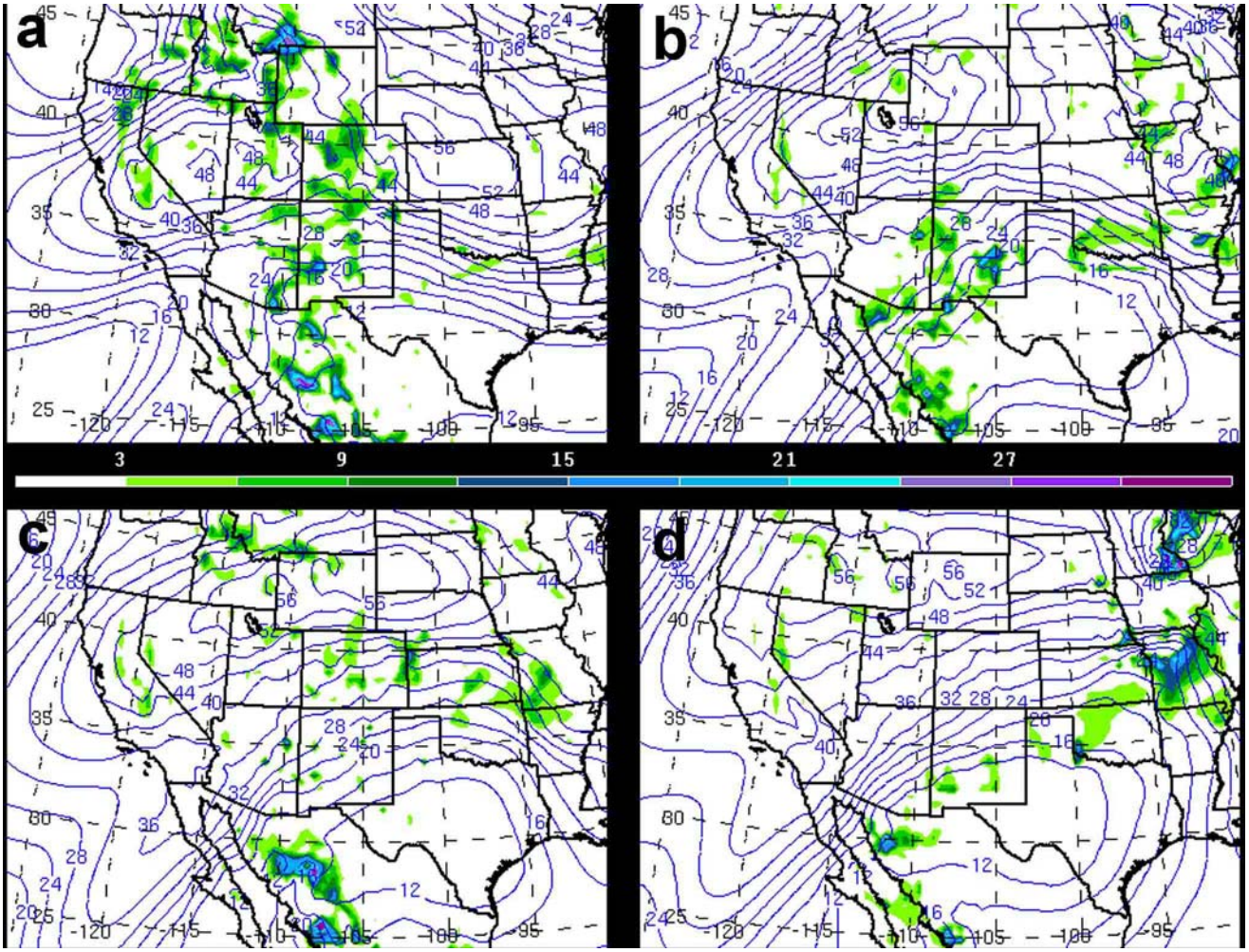

Fig 7. 300mb isotachs (contours, knts) and 500mb vertical velocity (shaded, cm/s) for the following times: a) 8 Aug 0000 UTC, b) 8 Aug 1200 UTC, c) 9 Aug 0000 UTC, and d) 9 Aug1200 UTC.

the western GP. Rainfall increases intensely over the SMO and covers more of a broad region to points downstream from the anti-cyclonic flow in this area large, There are also fewer localized regions of intense precipitation over the U.S. and an increased number of less intense systems that drop rainfall over a greater area.

4. CONCLUSIONS

From an examination of four days during a week-long monsoon surge event it appears that two different flow regimes may exist within the overall surge period. These different regimes are controlled by the large-scale flow associated with the Pacific coast trough, the passage of easterly waves, and the monsoon anti-cyclone. It is the strength and position of these features that determines the mechanism and location where precipitation systems form, develop, and propagate.

During the first two-day period of the examined surge event, the large-scale mid to upper level Pacific trough is rather weak compared to the second two-day period, and the monsoon anti-cyclone does not appear to be distinctly present. The mid-level flow from the Pacific is initially westerly to northwesterly over the southwest U.S. This regime tends itself to be less than favorable for a strong surge of monsoon moisture. The convection over the SMO is less active during this period and precipitation occurring over the GP is largely attributed to systems originating near the mountains of CO, as seen in the precipitation, vertical velocity, and PV fields. During this period, some precipitation originating over the SMO, does reach the US, but extends only as far north as northern Texas.

During the second two-day period the Pacific trough strengthens and shifts west and the monsoon anti-cyclone develops and shifts westward as well. This results in stronger southwesterly flow at mid and low-levels over the monsoon region, and a more uniform wind and PV field at the mid to upper levels. During this time there is an increase in convection and precipitation over the SMO and a decrease over CO. The moisture gradient region pushes east of CO and further north into AZ and NM. A region of high-valued PV air develops over the SMO in association with the increased convection, and this feature remains intact as it propagates across the central GP. The precipitation field is initially co-located with the PV anomaly, but the PV anomaly lags the region of precipitation upon

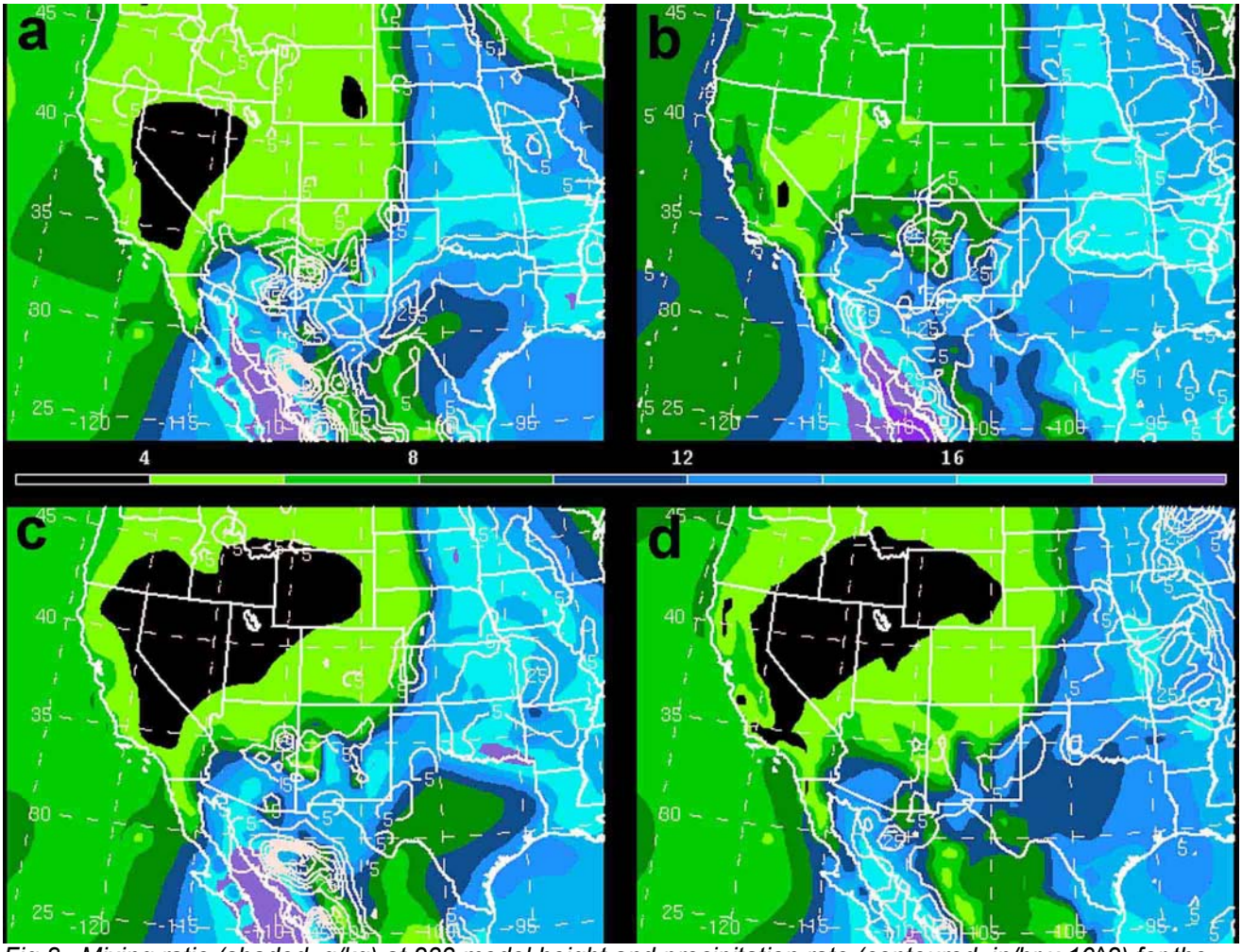

Fig 8. Mixing ratio (shaded, g/kg) at 233 model height and precipitation rate (contoured, in/hr x 10^2) for the following times: a) 8 Aug 0000 UTC, b) 8 Aug 1200 UTC, c) 9 Aug 0000 UTC, and d) 9 Aug1200 UTC.

propagation onto the east-central plains. Here the precipitation field is most prominent near the mid-level moisture and PV gradient region.

Other individual surge events vary in intensity and duration, but each of them is controlled to some degree by the large-scale mid-level monsoonal flow. Here we have simply tried to distinguish the different influences that the monsoon has on the central US depending upon the presence of a weak or strong monsoon surge period.

Acknowledgments. This research was supported by a grant from the National Oceanic and Atmospheric Administration under contract #NA17RJ1228.

5. REFERENCES

Badan-Dangon, A., C.E. Dorman, M.A. Merrifield, and C.D. Winant, 1991: The lower atmosphere over the Gulf of California. *J. Geophys. Res.*, **96(C9)**, 877-896.

Brenner, I. S., 1974: A surge of maritime tropical air – Gulf of California to the southwestern United States. *Mon. Wea. Rev.*, **102**, 375-389.

Bryson, R.A., and F.K. Hare, 1974: *The Climates of North America. World Survey of Climatology*. Vol. 11: *Climates of North America.* El-sevier, 1-45.

Douglas, M.W., 1993a: The summertime low-level jet over the Gulf of California: mean structure and synoptic variation. Preprints, *20th Conf. Hurricanes and Tropical Meteor.*, San Antonio, TX, Amer. Meteor. Soc., 504-507.

Douglas, M.W., R.A. Maddox, K. Howard, and S.Reyes, 1993: The Mexican Monsoon. *J. Climate*, **6**, 1665-1677.

Hales, J. E., Jr., 1972: Surges of maritime tropical air northward over the Gulf of California. *Mon. Wea. Rev.*, **100**, 298-306.

Jurwitz, L., 1953: Arizona's two-season rainfall pattern. *Weatherwise*, **6**, 96-99.

Mecikalski, J.R. and G.J. Tripoli, 1998: Inertial available kinetic energy and the dynamics of tropical plume formation. *Mon. Wea. Rev.*, **126**, 2200-2216.

Sadler, J.C., M.A. Lander, A.M. Hori, and L.K. Oda, 1987: *Tropical Marine Climatic Atlas: Vol. 2. Pacific Ocean*. Department of Meteorology, Atlas UHMET 87-02, University of Hawaii, 27 pp.

Stensrud, D.J., R. Gall, S.L. Mullen, and K.W. Howard, 1995: Model Climatology of the Mexican Monsoon. *J. Climate*, **8**, 1775-1794.

Stensrud, D.J., R.L. Gall, and M.K. Nordquist, 1997: Surges over the Gulf of California during the Mexican monson. *Mon. Wea. Rev.*, **125**, 417-437.

Walko, R.L, W.R. Cotton, J.L. Harrington, M.P. Meyers, 1995: New RAMS cloud microphysics parameterization. Part I: The single-moment scheme. *Atmos. Res.*, **38**, 29-62.